# Mistuning Effects on Flutter Margin

Roque Corral and Carlos Martel

January 25, 2012

**Abstract**

*A simple model is derived to describe the effect of mistuning on the stability properties of aerodynamically unstable rotors. The model assumes that both, the aerodynamics and the structural dynamics of the assembly are linear, and retains the first order terms of a fully consistent asymptotic expansion of the tuned system where the small parameter is the blade mistuning. The simplicity of the model allows the optimization of the blade mistuning pattern to achieve maximum rotor stability. The results of the application of this technique to realistic welded-in-pair and interlock low-pressure-turbine rotors are also presented.*

## 1 Introduction

Bladed discs used in turbine engines are nominally designed to be cyclically symmetric. However, in practice, small variations that result from the manufacturing process and wear break the symmetry, split the eigenvalue pairs and prevent the existence of travelling-wave modes. Numerous studies have been conducted to understand mistuning effects on the dynamics of bladed disc assemblies (see the survey paper of Srinivasan [1]). The main conclusions are that while mistuning has an undesirable effect on forced response, increasing the maximum amplitude of some blades, it has often a beneficial (stabilizing) effect on flutter (see Ref. [2])

There are numerical ([3, 2, 4], among others) and experimental [5] evidences that mistuning has a strong beneficial effect on self-excited vibrations. However recent attempts to analyse [6] or devise design methods [7] retaining the effect of flutter on mistuning are scarce and concentrated on fans.

Flutter has been a common problem for fans and compressors. Recently, due to the increasing relevance in terms of cost and weight of low-pressure-turbines (LPTs) in the architecture of modern large civil aero-engines, and the continuous trend to reduce them keeping the same efficiency, the stiffness of LPT rotor blades has been gradually reduced making them more flutter prone. It has been reported [8] that some LPTs may operate safely even if the rotor is aerodynamically unstable. However, it is evident that the design of LPT rotors may be constrained by flutter criteria and thus the seek of mechanisms to alleviate this problem is desirable.

Several authors have suggested to increase the design space of aerodynamically unstable rotors by using intentional mistuning [3, 2, 4, 9]. Although both natural and random mistuning increases the stability of the assembly the difference between the statistically minimum and maximum values of damping is large enough to favour the implementation of mechanisms that ensure values close to the statistically maximum damping.

The analysis of mistuned rotors usually leads to the use of either statistical or optimization methods [9] to obtain the worst mistuning pattern. In any case the need of reduced order models (ROMs) to reduce

the computational time is required. The simplest form of ROMs are lumped methods where the structure is modelled by mass-spring systems [10]. Lumped modes however provide a qualitative description of the dynamics of the assembly. To obtain a more accurate description finite element-based reduced order methods are required. During the last years two approaches based on a component mode synthesis and the use of a subset of nominal modes (SNM) have been developed. Methods based on component mode synthesis consider the blades and disk as separate sub-structures [11, 12], while the ones using SNM consider the bladed disk as a single structure [13].

Recently an extension of the SNM, known as the Fundamental Mistuning Model (FMM), that takes advantage of reducing the set of nominal modes to a single family has been developed [14]. The method only requires the natural frequencies and aerodynamic damping of the tuned system and has been used to predict the stability increase due to mistuning of LPT bladed disks [15].

This paper presents a further reduction of the FMM for cases in which all the modes of the family do not share the same frequency and mode-shape (apart from differences in the inter-blade phase angle). This is important for LPT bladed disks that feature either very flexible disks or inter-locked shrouds. The method is derived by means of a fully consistent asymptotic analysis of the mistuned rotor where the small parameter is the mistuning amplitude. The resulting model, referred to hereafter as Asymptotic Mistuning Model (AMM), is not significantly faster than the FMM but helps to uncover the basic physical mechanisms of mistuning since it accounts for only the minimum subset of degrees of freedom that play a relevant role in the mistuning process.

In this paper we will first review the methodology currently applied to compute the aerodynamic effects on the stability of tuned bladed disks, with special emphasis in its asymptotic character. Then we will describe the Asymptotic Mistuning Model and its application to mistuned rotors. And finally, the application of the AMM to increase the stability of two realistic bladed-disks (representative of an inter-locked and a welded-in-pair LPT rotor, see Fig. 1) using intentional mistuning will be presented.

## 2 Tuned System

The equations of motion for the small amplitude vibration of a perfectly tuned bladed disk with $N$ identical sectors, in the absence of any external forcing except for the linear aerodynamic effects, take the form

$$\mathbf{M}\ddot{\mathbf{x}} + \mathbf{K}\mathbf{x} = \mathbf{L}(\mathbf{x})_{\text{aero}}, \tag{1}$$

where the bladed disk degrees of freedom (after an appropriate FEM discretization) are stored in $\mathbf{x}(t)$, $\mathbf{M}$ and $\mathbf{K}$ are the mass and stiffness matrices, both symmetric and positive definite, and $\mathbf{L}_{\text{aero}}$ accounts for the aerodynamic forces. Structural damping has been neglected; the only source of damping considered in the formulation above is that coming from the aerodynamic terms, which is typically the dominating one, see e.g. [16].

The vibration modes of the system can be written using complex notation as

$$\mathbf{x} = \mathbf{X}\mathrm{e}^{\mathrm{i}\omega t} + \text{c.c.}, \tag{2}$$

where the vibration mode shape $\mathbf{X}$ and the mode oscillation frequency and damping $\omega$ (c.c. stands for the

complex conjugate) are given by the following eigenvalue problem

$$(\mathbf{K} - \omega^2 \mathbf{M})\mathbf{X} = \mathbf{M}_{\text{aero}}(\omega)\mathbf{X}, \tag{3}$$

which requires the knowledge of the matrix of aerodynamic forces $\mathbf{M}_{\text{aero}}$ as a function of $\omega$. The calculation of $\mathbf{M}_{\text{aero}}$ for a given $\omega$ value involves the solution of the linearized Navier-Stokes equations that prescribe the airflow around the blades for all linearly independent blade displacements. Therefore, the computation of the bladed disk vibration characteristics using the fully coupled structural-aerodynamic formulation given by Eqn. (3) is extremely costly and simply not realizable for any realistic configuration of practical interest.

The computational cost of this problem is drastically reduced if one takes into account the fact that the aerodynamic effects produce only small variations of the purely structural vibration frequencies. With this idea in mind, we will first rewrite Eqn. (3) using the structural mode basis and then apply an asymptotic perturbation method to obtain the first order aerodynamic correction of the purely structural vibration characteristics. This is a well known procedure to compute the aerodynamic stability properties of tuned bladed disks (see [17, 15] for a recent application of this approach in two and three dimensional configurations), but we will briefly outline it below because it constitutes a necessary previous step before the analysis of the mistuned case.

**Structural vibration modes.**

If the response vector (2) is partitioned as

$$\mathbf{X} = \begin{bmatrix} X_1 \\ X_2 \\ \vdots \\ X_N \end{bmatrix}, \tag{4}$$

with the vector $X_j$ containing the displacements of the $m$ degrees of freedom associated with sector $j$, then the problem that gives the natural oscillations of the tuned bladed disk without aerodynamic effects (Eqn. (3) with $\mathbf{M}_{\text{aero}} = 0$) takes the form

$$\left( \begin{bmatrix} K & K_c & 0 & \cdots & K_c^{\mathrm{T}} \\ K_c^{\mathrm{T}} & K & K_c & \cdots & 0 \\ & & \ddots & \ddots & \\ K_c & 0 & \cdots & K_c^{\mathrm{T}} & K \end{bmatrix} - \omega^2 \begin{bmatrix} M & M_c & 0 & \cdots & M_c^{\mathrm{T}} \\ M_c^{\mathrm{T}} & M & M_c & \cdots & 0 \\ & & \ddots & \ddots & \\ M_c & 0 & \cdots & M_c^{\mathrm{T}} & M \end{bmatrix} \right) \begin{bmatrix} X_1 \\ X_2 \\ \vdots \\ X_N \end{bmatrix} = \begin{bmatrix} 0 \\ 0 \\ \vdots \\ 0 \end{bmatrix}, \tag{5}$$

where the $m \times m$ sector stiffness and mass matrices $K$ and $M$ are symmetric and the coupling between adjacent sectors is represented by the coupling stiffness and mass matrices $K_c$ and $M_c$.

The cyclic symmetry of the bladed disk (that is composed of a sector repeated $N$ times and arranged periodically) is now evident in the matrices in Eqn. (5) that exhibit a block circulant structure, i.e., each row can be obtained from the previous one after a wrap-around forward block shift. The associated complex

eigenvectors

$$\begin{bmatrix} X_1 \\ \vdots \\ X_j \\ \vdots \\ X_N \end{bmatrix} = \begin{bmatrix} Z_k \mathrm{e}^{\mathrm{i}(\frac{2\pi k}{N})1} \\ \vdots \\ Z_k \mathrm{e}^{\mathrm{i}(\frac{2\pi k}{N})j} \\ \vdots \\ Z_k \mathrm{e}^{\mathrm{i}(\frac{2\pi k}{N})N} \end{bmatrix}, \quad \text{for} \quad k = 1 \dots N, \tag{6}$$

correspond to travelling waves with $k$ nodal diameters that, taking into account Eqn. (2), rotate around the annulus with constant angular velocity $\frac{\omega}{(2\pi k/N)}$. The complex vector $Z_k$ of size $m$ contains the mode shape details and the only eigenvector variation from sector to sector is just a phase increment of amount $\frac{2\pi k}{N}$(the so-called "interblade phase angle"). The vector $Z_k$ can be regarded as the $k$-th mode of the discrete Fourier transform of the $N$-periodic sequence of the sector degrees of freedom along the complete structure, $X_1, \dots X_N$; recall that the relation between Fourier modes $F_1, \dots F_N$ and sector degrees of freedom $S_1, \dots S_N$ is given by

$$S_j = \sum_{k=1}^{N} F_k \mathrm{e}^{\mathrm{i}(\frac{2\pi k}{N})j}, \quad \text{for} \quad j = 1 \dots N, \quad \text{and} \tag{7}$$

$$F_k = \frac{1}{N} \sum_{j=1}^{N} S_j \mathrm{e}^{-\mathrm{i}(\frac{2\pi j}{N})k}, \quad \text{for} \quad k = 1 \dots N. \tag{8}$$

Note also that it is enough to consider the value of $k$ modulo $N$; the change $k \to k + N$, that corresponds to the addition of a complete turn around the rotor, leaves all the above expressions unchanged.

If we now insert expression (6) into Eqn. (5), $N$ decoupled eigenvalue problems of size $m$ are obtained

$$\begin{gathered} ((K_c - \omega^2 M_c)\mathrm{e}^{\mathrm{i}(\frac{2\pi k}{N})} + (K_c - \omega^2 M_c)^{\mathrm{T}} \mathrm{e}^{-\mathrm{i}(\frac{2\pi k}{N})} + K - \omega^2 M) Z_k = 0, \\ \text{for} \quad k = 1 \dots N, \end{gathered} \tag{9}$$

which, for each $k$, have $m$ real eigenvalues, $\omega_{k1}^2, \dots, \omega_{km}^2 \geq 0$, that give the oscillation frequencies of the structure. The associated eigenvectors, $Z_{k1}, \dots, Z_{km}$, are, in general, complex and can be taken to be such that the square matrix

$$P_k = [Z_{k1} | Z_{k2} | ... | Z_{km}] \tag{10}$$

verifies

$$P_k^{\mathrm{H}} (M_c \, \mathrm{e}^{\mathrm{i}(\frac{2\pi k}{N})} + M_c^{\mathrm{T}} \mathrm{e}^{-\mathrm{i}(\frac{2\pi k}{N})} + M) P_k = I \quad \text{and} \tag{11}$$

$$P_k^{\mathrm{H}} (K_c \, \mathrm{e}^{\mathrm{i}(\frac{2\pi k}{N})} + K_c^{\mathrm{T}} \mathrm{e}^{-\mathrm{i}(\frac{2\pi k}{N})} + K) P_k = \Omega_k^2 = \begin{bmatrix} \omega_{k1}^2 & & 0 \\ & \ddots & \\ 0 & & \omega_{km}^2 \end{bmatrix}, \tag{12}$$

$$\text{for} \quad k = 1 \dots N,$$

that is, the eigenvectors are orthonormal with respect to the mass matrix and turn into diagonal form the sector stiffness matrix (the superindex $^{\mathrm{H}}$ stands for the conjugate transpose matrix), see e.g. [18]. Notice that the cyclic symmetry allows to drastically reduce the computational effort required to obtain the vibration modes of the tuned bladed disk: from $\mathcal{O}(N^3 m^3)$ for solving Eqn. (5) to only $\mathcal{O}(N m^3)$ for the $N$ eigenvalue problems in Eqn. (6).

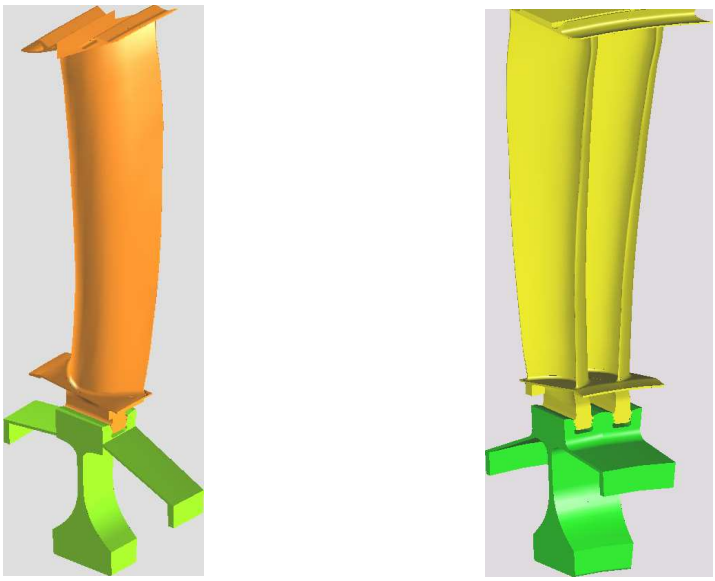

**Figure 1: GEOMETRY OF AN INTER-LOCK (LEFT) AND A WELDED-IN-PAIR (RIGHT) LPT BLADED-DISKS.**

The eigenvalue equation Eqn. (9) remains invariant under the changes

$$k \to N - k, \quad \omega_k^2 \to \omega_{N-k}^2 \quad \text{and} \quad Z_k \to \bar{Z}_{N-k}, \tag{13}$$

and thus, for every travelling wave rotating in one direction, there is also another identical one that rotates in the opposite direction with the same velocity. This symmetry comes from the fact that the original system (1) remains unchanged after time is reversed, $t \to -t$, because it does not exhibit any dissipation at all. Travelling wave modes come thus in counter-propagating pairs, except for those associated with $k = 0$ and $k = \frac{N}{2}$ (present only for $N = \dot{2}$), which have real $Z_k$ and can be seen as non propagative standing waves. Property (13) implies that the plot of the natural frequencies versus the number of nodal diameters, $k$, is symmetric, and only its first half (interblade phase angle from 0 to $\pi$) is normally plotted.

Figure 2 represents the natural frequencies of the purely structural problem, corresponding to a LPT rotor blade with an inter-locked shroud (left plot in Fig. 1) whose characteristics have been previously reported [15]. The main effect of inter-locking the rotor is twofold: first, it significantly raises the frequencies of the high nodal diameter modes, which in first approximation are torsion modes, and, second, it creates a region with a steep change in frequency that corresponds to shroud-dominated complex bending-torsion modes.

Figure 3 is the equivalent counter part for a welded-in-pair LPT rotor blade (right plot in Fig. 1). The geometry of both configurations is strictly the same and the differences between the modal characteristics are solely associated to the shroud boundary conditions. The frequency characteristics of this type of bladed-disks do not differ significantly from the ones with single cantilever rotor blades. Two regions may be clearly distinguished. First, a small region of disk dominated modes at low nodal diameters, which is an indication that the disk is very stiff compare to the blades. And, second, a large high nodal diameter region corresponding to flap "blade-alone" modes.

It is important to highlight that the steep variation of the natural frequencies seen in the shroud-dominated or disk-dominated nodal diameter region is characteristic of LPT bladed disks. Modern un-shrouded fans or

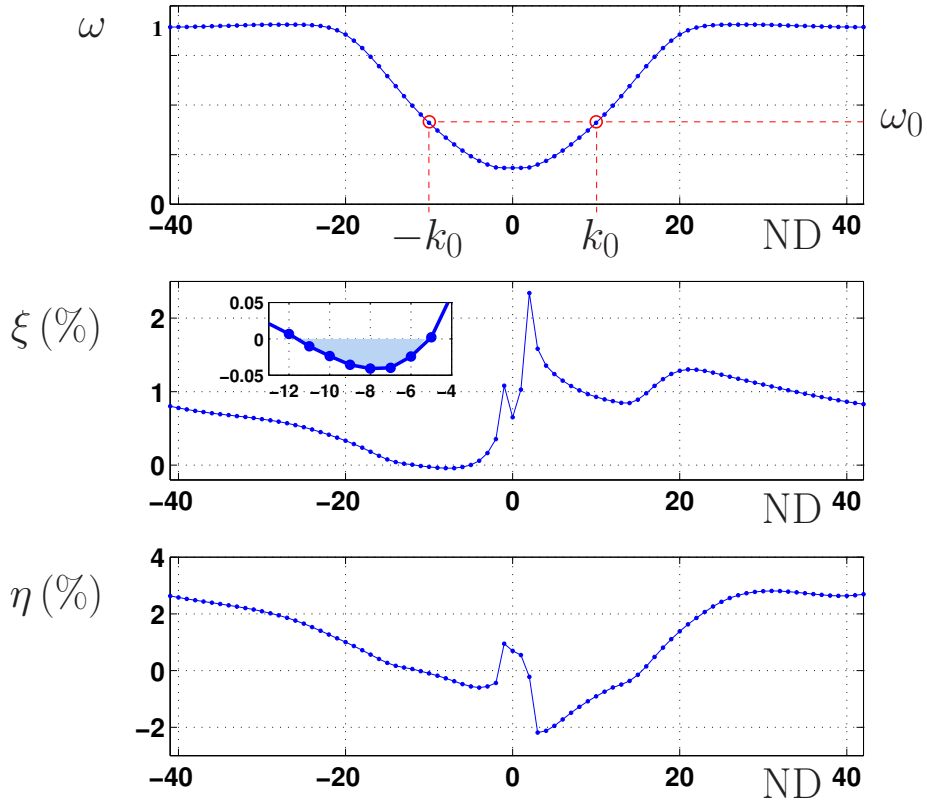


**Figure 2: TUNED VIBRATION CHARACTERISTICS VS. NUMBER OF NODAL DIAMETERS FOR THE FIRST FAMILY OF MODES OF AN INTER-LOCKED ROTOR [15] ($N = 84$). TOP: NORMALIZED VIBRATION FREQUENCY (ACTIVE MODES ENCIRCLED). MIDDLE: AERODYNAMIC DAMPING RELATIVE TO THE CRITICAL DAMPING. INSET: ZOOM OF THE UNSTABLE MODES (SHADING INDICATES INSTABILITY). BOTTOM: AERODYNAMIC FREQUENCY CORRECTION (SEE EQN. (23)).**

blisks exhibit frequency variations much smaller than the ones presented in this work, at least for the first families of modes.

### Aerodynamic correction.

In order to evaluate the aerodynamic correction of the vibration characteristics of the bladed disk it is convenient to first perform in Eqn. (3) the following change of variables to a purely structural travelling wave basis

$$\mathbf{X} = \mathbf{P}\mathbf{A}, \tag{14}$$

with

$$\mathbf{P} = \frac{1}{\sqrt{N}} \begin{bmatrix} P_1 \mathrm{e}^{\mathrm{i}(\frac{2\pi 1}{N})1} & \dots & P_N \mathrm{e}^{\mathrm{i}(\frac{2\pi N}{N})1} \\ \vdots & & \vdots \\ P_1 \mathrm{e}^{\mathrm{i}(\frac{2\pi 1}{N})j} & \dots & P_N \mathrm{e}^{\mathrm{i}(\frac{2\pi N}{N})j} \\ \vdots & & \vdots \\ P_1 \mathrm{e}^{\mathrm{i}(\frac{2\pi 1}{N})N} & \dots & P_N \mathrm{e}^{\mathrm{i}(\frac{2\pi N}{N})N} \end{bmatrix} \quad \text{and} \quad \mathbf{A} = \begin{bmatrix} A_1 \\ \vdots \\ A_j \\ \vdots \\ A_N \end{bmatrix}, \tag{15}$$

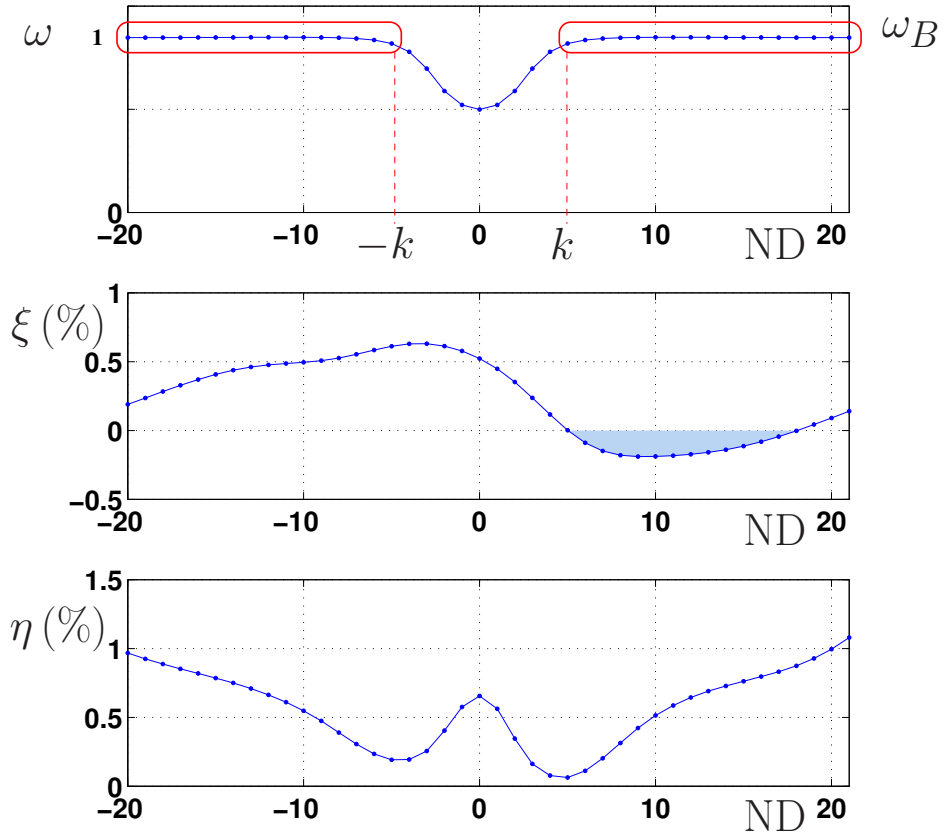


**Figure 3: TUNED VIBRATION CHARACTERISTICS VS. NUMBER OF NODAL DIAMETERS FOR THE FIRST FAMILY OF MODES OF A WELDED-IN-PAIR ROTOR [15] ($N = 42$). TOP: NORMALIZED VIBRATION FREQUENCY (ACTIVE MODES ENCIRCLED). MIDDLE: AERODYNAMIC DAMPING RELATIVE TO THE CRITICAL DAMPING (SHADING INDICATES INSTABILITY). BOTTOM: AERODYNAMIC FREQUENCY CORRECTION (SEE EQN. (23)).**

and where the vectors $A_j = [A_{j1}, \ldots, A_{jm}]^T$ contain the amplitudes of the different travelling wave modes. The eigenvalue problem in Eqn. (3) takes now the form

$$\begin{bmatrix} \Omega_1^2 - \omega^2 I & \ldots & 0 \\ \vdots & \ddots & \vdots \\ 0 & \ldots & \Omega_N^2 - \omega^2 I \end{bmatrix} \begin{bmatrix} A_1 \\ \vdots \\ A_N \end{bmatrix} = \mathbf{P}^{\mathrm{H}} \mathbf{M}_{\mathrm{aero}}(\omega) \mathbf{P} \begin{bmatrix} A_1 \\ \vdots \\ A_N \end{bmatrix}, \tag{16}$$

with diagonal mass and stiffness matrices, see Eqs. (11) and (12), and block diagonal aerodynamic matrix

$$\mathbf{P}^{\mathrm{H}} \mathbf{M}_{\mathrm{aero}}(\omega) \mathbf{P} = \begin{bmatrix} M_1(\omega) & \ldots & 0 \\ \vdots & \ddots & \vdots \\ 0 & \ldots & M_N(\omega) \end{bmatrix}, \tag{17}$$

as a result of the fact that the linearized aerodynamic flow problem has also cyclic symmetry and, therefore, the modes with different nodal diameters are completely independent.

The aerodynamic terms are small and give rise to a small correction of the purely structural vibration frequencies. For a given structural frequency $\omega_{\tilde{k}\tilde{j}}$ (corresponding to the $\tilde{j}$-th travelling wave mode with $\tilde{k}$ nodal diameters), its aerodynamically corrected counterpart $\omega$ is given by Eqn. (16), and it can be approximately estimated if one takes into account the following:

1. The modes with a different number of nodal diameters are decoupled and do not play any role in the correction of $\omega_{\tilde{k}\tilde{j}}$, that is,

$$A_k = 0, \quad \text{for all} \quad k \neq \tilde{k}. \tag{18}$$

2. The $\tilde{k}j$-th equation in Eqn. (16) reads

$$(\omega_{\tilde{k}j}^2 - \omega^2) A_{\tilde{k}j} = \sum_{h=1}^{m} [M_{\tilde{k}}(\omega)]_{jh} A_{\tilde{k}h}. \tag{19}$$

   The corrected frequency $\omega$ is close to $\omega_{\tilde{k}\tilde{j}}$, but not to the other frequencies $\omega_{\tilde{k}j}$ (we are implicitly assuming here that $\omega_{\tilde{k}\tilde{j}}$ is well apart from the rest of the frequencies corresponding to the same number of nodal diameters $\tilde{k}$). Therefore, if $j \neq \tilde{j}$ the term $(\omega_{\tilde{k}j}^2 - \omega^2)$ in the equation above is not small, but the aerodynamic terms, $[M_{\tilde{k}}(\omega)]_{jh}$, are small and we can neglect them to obtain

$$A_{\tilde{k}j} = 0, \quad \text{for all} \quad j \neq \tilde{j}. \tag{20}$$

   In other words, the rest of the travelling wave modes with $\tilde{k}$ nodal diameters and different frequencies do not contribute either to the correction of the $\omega_{\tilde{k}\tilde{j}}$ in first approximation.

3. And finally, taking into account (18) and (20), the $\tilde{k}\tilde{j}$-th equation in Eqn. (16) simplifies to

$$(\omega_{\tilde{k}\tilde{j}}^2 - \omega^2) A_{\tilde{k}\tilde{j}} = [M_{\tilde{k}}(\omega_{\tilde{k}\tilde{j}})]_{\tilde{j}\tilde{j}} A_{\tilde{k}\tilde{j}}, \tag{21}$$

   where the coefficients $(\omega_{\tilde{k}\tilde{j}}^2 - \omega^2)$ and $[M_{\tilde{k}}(\omega_{\tilde{k}\tilde{j}})]_{\tilde{j}\tilde{j}}$ are now both small, and we have also make use of the fact that $\omega$ is close to $\omega_{\tilde{k}\tilde{j}}$ to approximate

$$[M_{\tilde{k}}(\omega)]_{\tilde{j}\tilde{j}} = [M_{\tilde{k}}(\omega_{\tilde{k}\tilde{j}})]_{\tilde{j}\tilde{j}} + \cdots .$$

In summary, the shape of the purely structural vibration modes remains, in first approximation, unchanged by the aerodynamic effects, while the mode frequencies $\omega_{\tilde{k}\tilde{j}}$ experience a small correction that, according to Eq (21), can be expressed as

$$\omega = \omega_{\tilde{k}\tilde{j}}(1 - \frac{[M_{\tilde{k}}(\omega_{\tilde{k}\tilde{j}})]_{\tilde{j}\tilde{j}}}{2\omega^2_{\tilde{k}\tilde{j}}} + \cdots), \tag{22}$$

where the term $[M_{\tilde{k}}(\omega_{\tilde{k}\tilde{j}})]_{\tilde{j}\tilde{j}}$ represents the work of the aerodynamic forces over the blades, for a prescribed blade displacement that corresponds to the $\tilde{k}\tilde{j}$ vibration mode.

The computation of the work of the aerodynamic forces can be reduced to solving a set of linearized Navier-Stokes equations in a single sector with phase-shifted boundary conditions (see, e.g., [15, 17]). The resulting aerodynamic correction in Eqn. (22) is, in general, a complex number that can be written as

$$[M_{\tilde{k}}(\omega_{\tilde{k}\tilde{j}})]_{\tilde{j}\tilde{j}} = -2\omega^2_{\tilde{k}\tilde{j}}(\eta + \mathrm{i}2\xi), \tag{23}$$

where the real part $\eta$ represents a small relative correction of the oscillatory frequency and the (positive/negative) imaginary part $\xi$ is the small (stable/unstable) aerodynamic damping relative to the critical damping. The aerodynamic damping has to be evaluated for all system modes in order to know whether the bladed disk is stable or, on the contrary, some modes are unstable and flutter sets in. Moreover, the aerodynamic terms are not invariant under the changes in Eqn. (13), and, therefore, the aerodynamic correction for a pair of identical travelling waves that rotate in opposite directions is, in general, different and has to be separately computed.

Figures 2 and 3 (middle) represent the aerodynamic damping relative to the critical damping of the inter-lock and welded-in-pair configurations respectively. Both configurations are aerodynamically unstable however there are three very noticeable differences, namely,

1. The instability level of the inter-lock is much more moderated than the one of the welded-in-pair (for the same steady aerodynamics).
2. The unstable modes of the interlock are complex, shroud-dominated, bending-torsion modes while while in the welded-in-pair correspond to blade-alone, bending modes.
3. The unstable modes of the inter-lock rotor are located in a region of steep variation of the natural frequency, while the ones of the welded-in-pair rotor are located in a flat region in terms of frequency.

We will see that it is the third point the one that is relevant from point of view of the resulting AMM description. We will call the modes isolated or clustered depending on their relative difference in terms of frequency with the rest of the modes.

Figures 2 and 3 (bottom) show the frequency correction of the purely structural modes due to the aerodynamics. This correction is seldom taken into account in the standard design practice of LPT rotors. The average frequency correction for the inter-lock rotor due to the aerodynamics is about 2% while for the welded-in-pair is 1%, and the largest correction occurs for the highest nodal diameters.

# 3 Asymtotic Mistuning Model

The equations of motion for the vibration modes of a mistuned bladed disk with linear aerodynamic effects can be written as

$$((\mathbf{K} + \Delta\mathbf{K}) - \omega^2(\mathbf{M} + \Delta\mathbf{M}))\mathbf{X} = \mathbf{M}_{\mathrm{aero}}(\omega)\mathbf{X}, \tag{24}$$

which are simply the tuned equations (3) with the mistuning stiffness, $\Delta\mathbf{K}$, and mass, $\Delta\mathbf{M}$, matrices added. $\Delta\mathbf{K}$ and $\Delta\mathbf{M}$ are block diagonal matrices that contain the deviations from the mean stiffness $K$ and mass $M$ sector matrices (see Eqn. (5)), that is,

$$\Delta\mathbf{K} = \begin{bmatrix} \Delta K_1 & 0 & \cdots & 0 \\ 0 & \Delta K_2 & \cdots & 0 \\ & & \ddots & \\ 0 & 0 & 0 & \Delta K_N \end{bmatrix}, \quad \Delta\mathbf{M} = \begin{bmatrix} \Delta M_1 & 0 & \cdots & 0 \\ 0 & \Delta M_2 & \cdots & 0 \\ & & \ddots & \\ 0 & 0 & 0 & \Delta M_N \end{bmatrix}, \tag{25}$$

$$\text{with} \quad \textstyle\sum_{j=1}^{N} \Delta K_j = 0, \, \sum_{j=1}^{N} \Delta M_j = 0, \tag{26}$$

$$\text{and} \quad \Delta K_j = \Delta K_j^{\mathrm{T}}, \, \Delta M_j = \Delta M_j^{\mathrm{T}} \quad \text{for} \quad j = 1 \ldots N. \tag{27}$$

The mistuning of the sector coupling block matrices has not been included in the model above; the coupling matrices involve only a very small subset of the DOF of the sector and, thus, its mistuning is negligible as compared with that of the main sector.

As we did in the previous section, we first rewrite Eqn. (24) using the tuned travelling wave mode basis, Eqs. (14) and (15), to obtain

$$\begin{bmatrix} \Omega_1^2 - \omega^2 I & \ldots & 0 \\ \vdots & \ddots & \vdots \\ 0 & \ldots & \Omega_N^2 - \omega^2 I \end{bmatrix} \begin{bmatrix} A_1 \\ \vdots \\ A_N \end{bmatrix} = \mathbf{P}^{\mathrm{H}} \mathbf{M}_{\mathrm{aero}}(\omega) \mathbf{P} \begin{bmatrix} A_1 \\ \vdots \\ A_N \end{bmatrix} - \\ -\mathbf{P}^{\mathrm{H}} (\Delta\mathbf{K} - \omega^2 \Delta\mathbf{M}) \mathbf{P} \begin{bmatrix} A_1 \\ \vdots \\ A_N \end{bmatrix}, \tag{28}$$

where the aerodynamic matrix is block diagonal, see Eqn. (17). The structure of the mistuning correction matrix can be more easily analyzed if we make use of the Fourier modes of the sector distribution of the mistuning mass and stiffness, $\Delta K_k^{\mathrm{F}}$and $\Delta M_k^{\mathrm{F}}$, which, according to Eqn. (7), are given by

$$\Delta K_j = \sum_{k=1}^{N} \Delta K_k^{\mathrm{F}} \mathrm{e}^{\mathrm{i}(\frac{2\pi k}{N})j} \quad \text{and}$$

$$\Delta M_j = \sum_{k=1}^{N} \Delta M_k^{\mathrm{F}} \mathrm{e}^{\mathrm{i}(\frac{2\pi k}{N})j} \quad \text{for} \quad j = 1 \ldots N,$$

and verify (see Eqs. (26) and (27))

$$\Delta K_N^{\mathrm{F}} = 0, \; \Delta M_N^{\mathrm{F}} = 0 \quad \text{and} \quad \Delta K_k^{\mathrm{F}} = \overline{\Delta K_{-k}^{\mathrm{F}}}, \quad \Delta M_k^{\mathrm{F}} = \overline{\Delta M_{-k}^{\mathrm{F}}},$$
$$\Delta K_k^{\mathrm{F}} = (\Delta K_k^{\mathrm{F}})^{\mathrm{T}}, \; \Delta M_k^{\mathrm{F}} = (\Delta M_k^{\mathrm{F}})^{\mathrm{T}}, \quad \text{for} \quad k = 1 \ldots N. \tag{29}$$

After inserting the above expressions into Eqn. (28), the mistuning matrix takes the form

$$\mathbf{P}^{\mathrm{H}} (\Delta\mathbf{K} - \omega^2 \Delta\mathbf{M}) \mathbf{P} = \begin{bmatrix} 0 & \Delta_{12} & \ldots & \Delta_{1N} \\ \Delta_{21} & 0 & \ldots & \Delta_{2N} \\ \vdots & \vdots & \ddots & \vdots \\ \Delta_{N1} & \Delta_{N2} & \ldots & 0 \end{bmatrix}, \tag{30}$$

where each block is related to the Fourier components of the mistuning by

$$\Delta_{kj} = P_k^{\mathrm{H}}(\Delta K_{k-j}^{\mathrm{F}} - \omega^2 \Delta M_{k-j}^{\mathrm{F}})P_j, \tag{31}$$

and verifies

$$\Delta_{kj} = \Delta_{jk}^{\mathrm{H}}. \tag{32}$$

Note that the mistuning matrix in Eqn. (30) exhibits off diagonal blocks and, thus, mistuning couples travelling waves with different number of nodal diameters. Moreover, according to Eqn. (31), the coupling between the travelling waves with $k$ and $j$ nodal diameters takes place precisely through the $(k-j)$ Fourier mode of the mistuning.

The mistuning and aerodynamic effects are small and give rise to small corrections of the purely structural natural oscillation frequencies. We will now use exactly the same arguments as in the previous section in order to derive a set of simplified equations that allow us to obtain an estimate of the mistuning and aerodynamic correction $\omega$ of a given structural frequency $\tilde{\omega}$.

The solution $\omega$ of Eqn. (28) that we are looking for is close to $\tilde{\omega}$ and this allow us to distinguish between two different kinds of travelling wave modes:

1. Modes with frequencies that are not close to $\tilde{\omega}$ , that is, modes whose frequency $\omega_{kj}$ is such that $|\tilde{\omega} - \omega_{kj}|$ is large as compared with the typical aerodynamic and mistuning frequency corrections. The corresponding equation for this kind of modes in Eqn. (28) is of the form

$$(\omega_{kj}^2 - \omega^2)A_{kj} = \sum_{i,h=1}^{m} (\text{small terms})\ A_{ih},$$

where the coefficient in the left hand side is large as compared with the small aerodynamic and mistuning terms in the right hand side because $\omega$ is close to $\tilde{\omega}$ but not to $\omega_{kj}$. After neglecting the small terms, the equation above yields

$$A_{kj} = 0, \tag{33}$$

and, as it was already obtained in item 2 of the previous section, all travelling wave modes with frequencies well apart from $\tilde{\omega}$ do not contribute in first approximation to its correction.

2. And modes with frequencies close to $\tilde{\omega}$ , i.e., with frequencies that are at a distance from $\tilde{\omega}$ of the same order of the small aerodynamic and mistuning frequency corrections. We will hereafter refer to these modes as "active" modes because they are, in first approximation, the only ones that take part in the correction of $\tilde{\omega}$. After removing the not active modes of the previous item from Eqn. (28), the resulting equation for an active mode with amplitude $A_a$ and tuned structural frequency $\omega_a$ reads

$$(\omega_a^2 - \omega^2)A_a = -2\omega_a^2(\eta_a + \mathrm{i}2\xi_a)A_a - \sum_{a' \neq a} \delta_{aa'} A_{a'}, \tag{34}$$

where all coefficients are now small. The aerodynamic term was obtained in the previous section, the sum goes over all active modes except $A_a$ and, according to Eqn. (31), the mistuning coupling coefficients can be written as

$$\delta_{aa'} = Z_a^{\mathrm{H}}(\Delta K_{k-k'}^{\mathrm{F}} - \tilde{\omega}^2 \Delta M_{k-k'}^{\mathrm{F}})Z_{a'}, \tag{35}$$

where $Z_a$, $Z_{a'}$, $k$ and $k'$ are, respectively, the mode shapes and the number of nodal diameters of the

active modes $A_a$ and $A_{a'}$, and the frequency $\omega$ has been approximated by $\tilde{\omega}$ (note also that the mistuning coupling terms verify $\delta_{aa'} = \overline{\delta_{a'a}}$ because mistuning constitutes a purely structural, conservative perturbation). And finally, we introduce the frequency correction $\omega = \tilde{\omega}(1 + \Delta\omega)$ (with $|\Delta\omega| \ll 1$), in order to write Eqn. (34) in the more convenient form

$$((\omega_a^2 - \tilde{\omega^2}) - 2\tilde{\omega^2}\Delta\omega)A_a = -2\omega_a^2(\eta_a + \mathrm{i}2\xi_a)A_a - \sum_{a' \neq a} \delta_{aa'} A_{a'}. \tag{36}$$

In a general situation, we have as many equations like Eqn. (36) as active modes, which form a reduced eigenvalue problem that allow us to estimate correction of the frequencies close to $\tilde{\omega}$. We call this reduced problem the Asymptotic Mistuning Model (AMM) because the above described procedure can be seen as an asymptotic perturbation expansion in which we have computed only first correction term. The small parameters in this expansion are the size of the aerodynamic correction ($\sim$1%-2% in the examples shown in Figs. 2 and 3) and the mistuning amplitude, which is considered of the same order: the smaller the aerodynamic and mistuning effects, the better the approximation given by the AMM.

The AMM description retains only the minimal set of travelling wave modes that are relevant for the estimation of the correction of a given purely structural, tuned frequency (and the nearby ones) due to aerodynamic and mistuning effects. It also reveals the coupling mechanism of mistuning: the only mistuning modes that are relevant are those that couple active modes, i.e., those modes with wavenumber equal to the difference of the number of nodal diameters of two active modes (see Eqn. (35)).

In the next section we focus on two frequent bladed disk modal configurations in order to illustrate the use of the AMM formulation and its capability to provide a simplified description of the combined effect of aerodynamics and mistuning on the linear stability characteristics.

# 4 Applications

The AMM has been used to determine the optimal mistuning pattern required for the stabilisation of two bladed-disks. Their frequency characteristics have been obtained using a finite-element model. The unsteady aerodynamics has been computed assuming that its influence is negligible in the structural modes. The purely structural mode-shapes and natural frequencies have been injected in a linearized Navier-Stokes solver and the unsteady aerodynamics associated to each mode-shape computed[15].

It has already been mentioned that the two cases have been carefully chosen to represent to different problems: the aerodynamic instability of an inter-lock and a welded-in-pair LPT bladed-disks. Both cases are substantially different because since in the former the unstable modes are separated in terms of frequency from the rest of the modes, in the latter there is a cluster of modes that share nearly the same frequency.

## Isolated modes

For the family of modes represented in Fig. 2, the marked vibration frequency $\omega_0$ is well apart from the rest, i.e., its distance to the rest of the frequencies is large as compared with the corresponding aerodynamic corrections (represented in the lower plots of Fig. 2). In this case, in order to take into account the effect of the mistuning it is enough to consider the two counter-rotating wavetrains with frequency $\omega_0$ and nodal diameters $\pm k_0$. In other words, these two modes are the only active modes in the AMM description, which

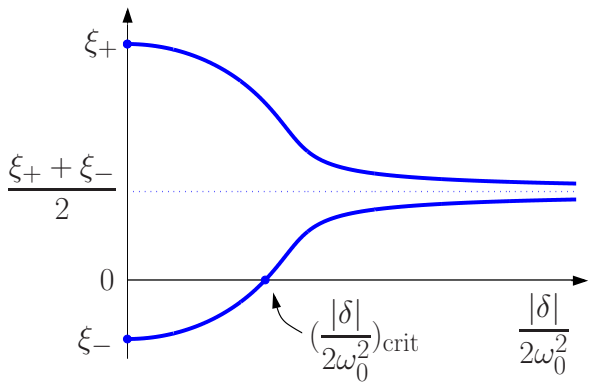


**Figure 4: DAMPING VARIATION FOR A PAIR OF ISOLATED MODES AS THE MISTUNING AMPLITUDE $|\delta|$ IS INCREASED.**

now takes its simplest form

$$\begin{aligned} -2\omega_0^2\Delta\omega A_+ &= -2\omega_0^2(\eta_+ + \mathrm{i}2\xi_+)A_+ - \delta A_-, \\ -2\omega_0^2\Delta\omega A_- &= -2\omega_0^2(\eta_- + \mathrm{i}2\xi_-)A_- - \bar{\delta} A_+, \end{aligned} \tag{37}$$

where $A_\pm$, $\eta_\pm$ and $\xi_\pm$ are, respectively, the amplitude, the relative aerodynamic correction frequency and damping of the $\pm k_0$ modes. The mistuning correction of the stability characteristics takes place only through its $2k_0$ Fourier mode,

$$\delta = Z^{\mathrm{H}}_{k_0}(\Delta K^{\mathrm{F}}_{2k_0} - \omega_0^2 \Delta M^{\mathrm{F}}_{2k_0})\overline{Z_{k_0}}. \tag{38}$$

The eigenvalue problem (37) can be explicitly solved to give

$$\Delta\omega = \frac{(\eta_+ + \eta_-) + 2\mathrm{i}(\xi_+ + \xi_-)}{2} \pm \sqrt{(\frac{(\eta_+ - \eta_-) + 2\mathrm{i}(\xi_+ - \xi_-)}{2})^2 + \frac{|\delta|^2}{4\omega_0^4}},$$

and, if we now decompose the frequency correction as $\Delta\omega = \eta + 2\mathrm{i}\xi$, the resulting mistuned relative critical dampings can be expressed as

$$\begin{aligned} \xi &= \frac{(\xi_+ + \xi_-)}{2} \pm \frac{1}{2}\sqrt{\frac{\sqrt{a^2+b^2} - a}{2}}, \quad \text{with} \\ a &= \frac{(\eta_+ - \eta_-)^2}{4} - (\xi^+ - \xi^-)^2 + \frac{|\delta|^2}{4\omega_0^4} \quad \text{and} \\ b &= (\eta^+ - \eta^-)(\xi^+ - \xi^-), \end{aligned}$$

which are plotted in Fig. 4 as functions of the mistuning amplitude $|\delta|$.

As it can appreciated from Fig. 4, in the absence of mistuning the tuned aerodynamic stability characteristics are recovered (one of the modes is stable $\xi_+ > 0$ and the other unstable and $\xi_- < 0$, see Fig. 2). When the mistuning size is increased both dampings approach the tuned average damping $\frac{(\xi_+ + \xi_-)}{2}$ (in fact, the average of the mistuned dampings remains constant and equal to its tuned value). The shape of the curve in Fig. 4 is completely similar to that obtained via numerical optimization in [9]. There is an initial region for small mistuning with very little change in the stability margin, then comes a region of stability variation due to mistuning and, finally, the sensitivity to mistuning decays again as mistuning is increased and the asymptotic

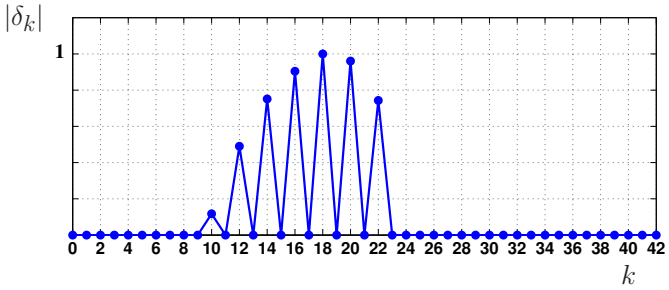


**Figure 5: FOURIER COEFFICIENT DISTRIBUTION OF THE MISTUNING PATTERN REQUIRED TO STABILIZE THE MODE FAMILY IN FIG. 2 ACCORDING TO EQN. (39).**

limit of stability is approached.

The mistuning is always stabilizing, but the stability increase of the unstable mode reduces the stability of the stable one. For positive averaged damping, i.e., for $\frac{(\xi_+ + \xi_-)}{2} > 0$, both modes can be stabilized just by increasing the mistuning above the critical value

$$(\frac{|\delta|}{2\omega_0^2})_{\text{crit}} = \sqrt{-\xi_+\xi_-(4 + \frac{(\eta_+ - \eta_-)^2}{(\xi_+ + \xi_-)^2})}. \tag{39}$$

On the other hand, if the averaged damping is negative, then the stabilization through a small intentional mistuning is not possible.

The expression for the mistuning coefficient given in Eqn. (38) can be easily interpreted in terms of the vibration frequency splitting produced by the mistuning when no aerodynamics effects are present. In this purely structural vibration case, the corrections of the frequency are given by Eqn. (37) with $\xi_\pm = 0$ and $\eta_\pm = 0$ that yields

$$\Delta\omega = \pm\frac{|\delta|}{2\omega_0^2},$$

and thus the size of the relative frequency splitting due to mistuning is precisely $|\delta|/\omega_0^2$. Now, going back to the critical mistuning in Eqn. (39), we can conclude that the mistuning required to achieve stabilization is the one that, in the absence of any aerodynamic effect, gives rise to a frequency splitting equal to twice the value in Eqn. (39).

Note also that the only relevant mistuning component is its $2k_0$ Fourier mode, and that Eqn. (38) indicates that, in order to be effective, the inclusion of intentional mistuning (via e.g., the addition of small masses) should take place in the sector regions with large local alternate stresses.

Finally, concerning the mode family depicted in Fig. 2, the unstable modes, which correspond to $k = -11, -10, -9, -8, -7, -6, -5$ (see the inset in the middle plot of Fig. 2), belong to isolated mode pairs and, according to the above results, can be stabilized just by the addition of a small mistuning pattern with the following six Fourier modes: $10, 12, 14, 16, 18, 20, 22$ (the resulting normalized profile of the Fourier coefficient distribution of the mistuning pattern required to achieve stabilization according to Eqn. (39) is represented in Fig. 5). The remaining modes simply do not play any role, in first approximation, in the mistuning process.

Another interesting conclusion is that alternate mistuning, which has been argued to be subopimal [9], has no effect on this type of configurations. This somehow more surprising if we consider that one of the few experimental attempts to assess the effect of mistuning on the aerodynamic damping of LPT airfoils (Ref. [5]) was performed using alternate mistuning.

## Clustered modes

A frequency distribution like the one plotted in Fig. 3, in which the natural frequencies of a family of modes approach fast a constant value, $\omega_B$, as the number of nodal diameters is increased, is frequently obtained in the vibration analysis of realistic tuned bladed disks. The frequency $\omega_B$ typically corresponds to a blade alone natural vibration frequency and the AMM description permits again to easily compute the mistuning induced corrections of the frequency and damping.

In this case, the group of active modes are those with $k$ or more nodal diameters (see Fig. 3), and we thus have $N_a = N - 2k + 1$ active modes, where $N$ is the number of sectors of the bladed disk. The AMM formulation simplifies this problem to the computation of the eigenvalues $\Delta\omega$ of a matrix of size $N_a$ that, according to Eqn. (36), can be written in the form

$$\begin{bmatrix} d_k & & & & \\ & d_{k+1} & & \Delta & \\ & & \ddots & & \\ & \Delta^{\mathrm{H}} & & d_{-(k+1)} & \\ & & & & d_{-k} \end{bmatrix} \begin{bmatrix} A_k \\ A_{k+1} \\ \vdots \\ A_{-(k+1)} \\ A_{-k} \end{bmatrix} = 0, \tag{40}$$

where the active modes have been ordered consecutively in $k$ (recall that the number of nodal diameters has to be considered only modulo $N$) and the diagonal elements are given by

$$d_j = (\omega_j^2 - \omega_B^2) + 2\omega_j^2(\eta_j + \mathrm{i}2\xi_j) - 2\omega_B^2\Delta\omega. \tag{41}$$

The sub and superdiagonal mistuning terms ($\Delta$ in the matrix above) can be further simplified if one takes into account that, in the almost constant frequency region that we are describing, the different mode shapes are approximately equal to that of the blade alone mode but with a different sector to sector phase change (i.e., a different interblade phase angle). That is, after arranging the blade and disk sector DOFs in the form

$$X_j = \begin{bmatrix} X_j^{\mathrm{blade}} \\ X_j^{\mathrm{disk}} \end{bmatrix},$$

the $j$ sector displacement associated with the $k$ mode can be approximately written as

$$X_j = \begin{bmatrix} Z_B \\ 0 \end{bmatrix} \mathrm{e}^{\mathrm{i}(\frac{2\pi k}{N})j},$$

where the real vector $Z_B$ contains the displacements of the blade alone mode with frequency $\omega_B$. This implies that the Fourier components of the modes in this near constant frequency region are equal and real,

$$Z = \begin{bmatrix} Z_B \\ 0 \end{bmatrix}, \tag{42}$$

and that the mistuning terms (see Eqn. (35)) can be reduced to

$$\delta_{kk'} = Z^{\mathrm{T}}(\Delta K^{\mathrm{F}}_{k-k'} - \omega_B^2 \Delta M^{\mathrm{F}}_{k-k'})Z. \tag{43}$$

The above expression for the mistuning terms depends only on $(k - k')$ and allow us to write the eigenvalue

problem (40) as

$$\begin{bmatrix} d_k & \delta_1 & \delta_2 & \dots & \delta_{N_a-1} \\ \overline{\delta_1} & d_{k+1} & \delta_1 & \dots & \delta_{N_a-2} \\ & & \ddots & & \\ \overline{\delta_{N_a-2}} & \dots & & d_{-(k+1)} & \delta_1 \\ \overline{\delta_{N_a-1}} & \dots & & \overline{\delta_1} & d_{-k} \end{bmatrix} \begin{bmatrix} A_k \\ A_{k+1} \\ \vdots \\ A_{-(k+1)} \\ A_{-k} \end{bmatrix} = 0, \tag{44}$$

where the mistuning appears only through the complex numbers $\delta_1, \delta_2, \dots, \delta_{N_a-1}$.

Proceeding as in [14], it is possible to relate the mistuning coefficients $\delta_k$ to the mistuned blade alone frequencies of the blades $\omega_{Bj}$ . To this end we assume that the blade alone mode shapes of the mistuned blades,

$$Z_j = \begin{bmatrix} Z_{Bj} \\ 0 \end{bmatrix},$$

are very close to that of the tuned blade in Eqn. (42) and then, in first approximation, we have

$$Z^{\mathrm{T}}(\Delta K_j - \omega_B^2 \Delta M_j) Z = Z^{\mathrm{T}}((K + \Delta K_j) - \omega_B^2 (M + \Delta M_j)) Z \simeq \\ \simeq Z_j^{\mathrm{T}}((K + \Delta K_j) - \omega_B^2 (M + \Delta M_j)) Z_j = \omega_{Bj}^2 - \omega_B^2, \tag{45}$$

where we have make use of the fact that $\omega_B$ and $Z_B$ in in Eqn. (42) are the blade alone frequency and mode shape of the tuned blade thus verify

$$Z^{\mathrm{T}}(K - \omega_B^2 M) Z = (\omega_B^2 - \omega_B^2) I = 0.$$

If we now introduce the blade alone mistuned frequency relative variation, $\Delta\omega_{Bj}$, given by

$$\omega_{Bj} = \omega_B (1 + \Delta\omega_{Bj}) \quad \text{with} \quad |\Delta\omega_{Bj}| \ll 1,$$

Eqn. (45) can be further simplified to

$$Z^{\mathrm{T}}(\Delta K_j - \omega_B^2 \Delta M_j) Z \simeq 2\omega_B^2 \Delta\omega_{Bj},$$

and then, the $\delta_k$ coefficients in Eqn. (44) can be written as

$$\delta_k = 2\omega_B^2 \Delta\omega_{Bk}^{\mathrm{F}},$$

where $\Delta\omega_{Bk}^{\mathrm{F}}$ is the $k$-th Fourier mode of the mistuned blade alone relative frequency variation pattern.

After collecting all the above results, the eigenvalue problem produced by the AMM formulation takes the final form

$$\begin{bmatrix} \tilde{d}_k & \Delta\omega_{B1}^{\mathrm{F}} & \Delta\omega_{B2}^{\mathrm{F}} & \dots & \Delta\omega_{BN_a-1}^{\mathrm{F}} \\ \overline{\Delta\omega_{B1}^{\mathrm{F}}} & \tilde{d}_{k+1} & \Delta\omega_{B1}^{\mathrm{F}} & \dots & \Delta\omega_{BN_a-2}^{\mathrm{F}} \\ & & \ddots & & \\ \overline{\Delta\omega_{BN_a-2}^{\mathrm{F}}} & \dots & \overline{\Delta\omega_{B1}^{\mathrm{F}}} & \tilde{d}_{-(k+1)} & \Delta\omega_{B1}^{\mathrm{F}} \\ \overline{\Delta\omega_{BN_a-1}^{\mathrm{F}}} & \dots & & \overline{\Delta\omega_{B1}^{\mathrm{F}}} & \tilde{d}_{-k} \end{bmatrix} \begin{bmatrix} A_k \\ A_{k+1} \\ \vdots \\ A_{-(k+1)} \\ A_{-k} \end{bmatrix} = 0, \tag{46}$$

where the diagonal elements can be written, in first approximation, as

$$\tilde{d}_j = \frac{(\omega_j^2 - \omega_B^2)}{2\omega_B^2} + (\eta_j + \mathrm{i}2\xi_j) - \Delta\omega, \tag{47}$$

and the mistuning terms verify $\Delta\omega_{Bk}^{\mathrm{F}} = \overline{\Delta\omega_{BN-k}^{\mathrm{F}}}$, because they come from the Fourier transform of a real sequence (see Eqn. (29)). Note that in this case the AMM can be seen as a simplification of the FMM [14], which takes into account a complete family of modes. The AMM includes only the active modes of the family and the final problem is smaller in size, with an associated matrix (see Eqn. (46) ) that is a submatrix of the one that is obtained from the FMM [15].

It is also interesting to mention that, as it happened in the isolated modes case, the resulting averaged damping remains constant and equal to its tuned value

$$\frac{1}{N_a}\sum_k \frac{\mathrm{Im}(\Delta\omega_k)}{2} = \frac{1}{N_a}\sum_k \xi_k, \tag{48}$$

where the sums go over all active modes, $\Delta\omega_k$ are the eigenvalues from Eqn. (46), and the mistuned dampings are given by $\frac{\mathrm{Im}(\Delta\omega_k)}{2}$. This invariance follows from the basic linear algebra property that states that the sum of the eigenvalues of a matrix is equal to its trace, and indicates that the increase of stability of a mode inevitably reduces the stability of other modes. Moreover, this property allow us to conclude that if the average of the tuned dampings is negative, then it is not possible to achieve complete stabilization through the inclusion of small mistuning.

The AMM formulation above is now used to look for the optimal mistuning patterns that stabilize the rotor in Fig. 3. The total number of sectors is $N = 42$ and we now have $N_a = 33$ active modes (all those with $|k| > 5$ encircled in red in the top plot of Fig. 3).

For every value of $|\Delta\omega_{Bk}^{\mathrm{F}}|_{\max}$, we use a a numerical optimization method to locate the mistuning pattern with Fourier coefficients below $|\Delta\omega_{Bk}^{\mathrm{F}}|_{\max}$ that maximizes the minimum damping (i.e., the mistuning pattern that gives maximum stabilization). The results are presented in Fig. 6, where it can be appreciated that complete stabilization can be achieved from $|\Delta\omega_{Bk}^{\mathrm{F}}|_{\max} \sim 0.2\%$ on. The Fourier modes of the resulting optimal mistuning patterns at several different stages of the optimization process are plotted in Fig. 7. The optimal mistuning pattern grows with $|\Delta\omega_{Bk}^{\mathrm{F}}|_{\max}$ but its mode distribution appears to relax to a profile where the most important contributions are approximately located: (i) around $k = 18$ that, as it can be seen from Fig. 6, corresponds to couplings between the most unstable and the most stable modes, and (ii) from $k = 1$ to $k = 9$, which can be related to the coupling only among the unstable modes and only among the stable modes.

# 5 Concluding Remarks

The derivation of a new reduced order model (Asymptotic Mistuning Model) based on the use of a subset of nominal modes has been presented. The method is, from a practical point of view, similar to the FMM, but they differ on three important points

1. The AMM is derived recurring solely to the use of asymptotic perturbation techniques.
2. The AMM uses only the active modes of a given family of modes, i.e.: those who are relevant from the point of view of mistuning, and in this sense is more reduced than the FMM. Its simplicity unveils

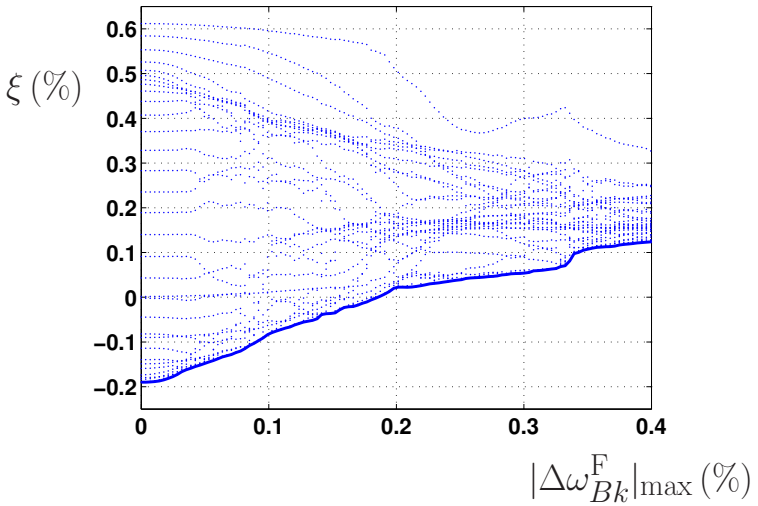


**Figure 6: CRITICAL DAMPING OF THE OPTIMUM MISTUNED CONFIGURATION FOR THE ACTIVE MODES INDICATED IN Fig. 3 AS A FUNCTION OF THE MAXIMUM BLADE ALONE FREQUENCY DEVIATION $|\Delta\omega^{\mathbf{F}}_{Bk}|_{\mathbf{max}}$. THICK LINE: MINIMUM DAMPING ENVELOPE. DOTTED LINES: DAMPING OF ALL ACTIVE MODES.**

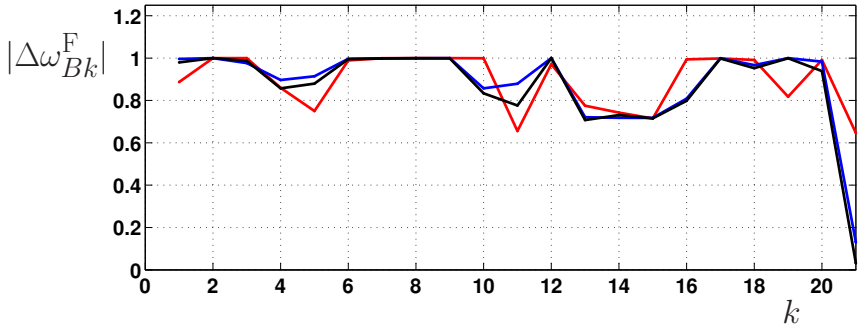


**Figure 7: NORMALIZED FOURIER COEFFICIENTS OF THE OPTIMAL BLADE FREQUENCY DEVIATION PATTERNS FOR SEVERAL DIFFERENT MAXIMUM BLADE ALONE FREQUENCY DEVIATIONS IN FIG. 6, $|\Delta\omega^{\mathbf{F}}_{Bk}|_{\mathbf{max}} = .2, .3$ AND $.4$ (RED, BLUE AND BLACK LINES RESPECTIVELY).**

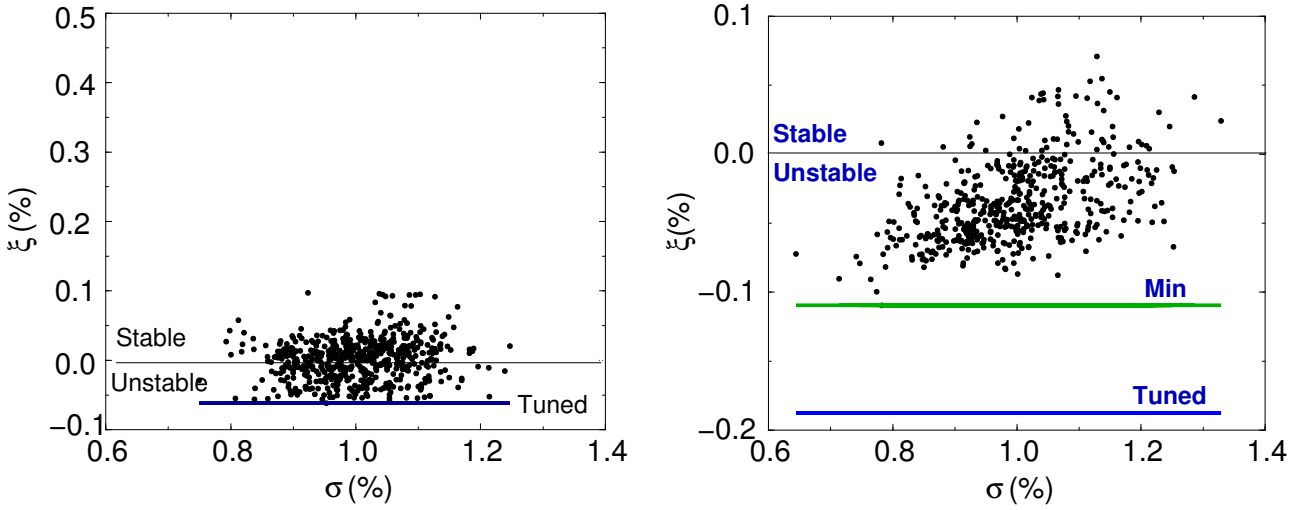


**Figure 8: MINIMUM DAMPING AS A FUNCTION OF THE STANDARD DEVIATION, $\sigma$, OF THE NATURAL FREQUENCIES OF AN INTER-LOCK (LEFT) AND A WELDED PAIR (RIGHT) BLADED DISK (TAKEN FROM REF. [15])**

the physical mechanism of the mistuning induced coupling between different travelling-wave modes and provides valuable information on how to use intentional mistuning in order to increase the stability of aerodynamically unstable rotors.

3. The AMM may be used to deal with isolated modes as the ones that may be encountered on welded-in-pair and interlocked LPT bladed-disks. It may be noticed that the consistent application of the FMM is restricted only to problems in which the variation of the natural frequencies of the family modes is very small and their mode shapes differ just in the inter-blade phase angle in first approximation.

The method has been used to increase the stability of two aerodynamically unstable LPT rotors. The first case corresponds to a rotor with an inter-locked shroud. The unstable modes correspond to separated modes and the AMM provides an analytical description of the optimum mistuning pattern. The second case is representative of a welded-in-pair rotor. The unstable modes are clustered about a single frequency and an optimization process is conducted in order to find the optimum mistuning pattern.

As a final remark, it is interesting to comment the work in Ref. [15] on the effect of random mistuning on the aerodynamic stability of the Inter-locked and Welded-in-pair bladed disks in Figs. 2 and 3. Their results indicate that the minimum damping remains unaffected (and equal to its tuned value) for the Interlock case while, for the Welded-in-pair rotor, there is a clear increase of the minimum damping (i.e., a clear stabilization). This can be appreciated from Fig. 8 where the minimum damping, $\xi$, is plotted for a population of random mistuning patterns ($\sigma$ is the standard deviation of the frequencies of the mistuning patterns). These two different responses to random mistuning can be explained using the AMM results form the previous section: The increase on the stability of one of the isolated unstable, e.g. $k = -8$, modes in the Interlock mode family in Fig. 2 takes place precisely only through the $k = 16$ mode of the mistuning, which induces a coupling with the $k = 8$ stable mode. On the other hand, the stability of one of the unstable modes, $k = 10$ for instance, of the Welded-pair family in Fig. 3 is increased by the effect of many mistuning modes (approximately all modes from $k = 9$ to $k = 36$ modulo 42) that provide coupling with the rest of stable active modes. Therefore, an increase of stability as a result of a random mistuning pattern is much more probable for the Welded-pair family, and this is what is reflected in the plots in Fig. 8.

# References


[1] Srinivasan, A., 1984. "Vibrations of bladed-disc assemblies: A selected survey". *Journal of Vibration, Stress, and Reliability on Design,* **106**(2), pp. 165–168.

[2] Kaza, K., and Klieb, R., 1982. "Flutter and response of a mistuned cascade in incompressible flow". *AIAA Journal,* **20**(8), pp. 1120–1127.

[3] Srinivasan, A., 1980. "Influence of mistuning on blade torsional flutter". *NASA CR-165137*(1), August.

[4] Bendiksen, O., 1984. "Flutter of mistuned turbomachinery rotors". *Journal of Engineering for Gas Turbines and Power,* **106**, January, pp. 25–33.

[5] Nowinsky, M., and Panovsky, J., 2000. "Flutter mechanisms in low pressure turbine blades". *Journal of Engineering for Gas Turbines and Power,* **122**, pp. 82–88.

[6] Sadeghi, M., and Liu, F., 2001. "Computation of mistuning effects on cascade flutter". *AIAA Journal,* **39**(1), pp. 22–28.

[7] Seinturier, E., Dupont, C., Berthillier, M., and Dumas, M., 2002. "A new method to predict flutter in presence of structural mistuning with application to a wide chord fan stage". *presented at the 9th International Symposium on Unstaedy Aerodynamics, Aeroacoustics and Aeroelasticity of Turbomachines*, pp. 739–749.

[8] Corral, R., and Gallardo, J., 2005. "Strain-gauge prediction of self-excited vibrations on low pressure turbine blades". *presented at the AVT-121 RTO symposium on Evaluation, Control and Prevention of High Cycle Fatigue in Gas Turbine Engines for Land, Sea and Air, Granada, Spain.*

[9] Crawley, E., and Hall, K., 1985. "Optimization and mechanisms of mistuning in cascades". *Journal of Engineering for Gas Turbines and Power,* **107**, April, pp. 418–426.

[10] Ewins, D., 1969. "The effects of detuning upon the forced vibrations of bladed-disks". *Journal of Sound Vibration,* **9**(1), pp. 65–79.

[11] Yang, M.-T., and Griffin, J., 1997. "A reduced order approach for the vibration of mistuned nalded disk assemblies". *Journal of Engineering for Gas Turbines and Power,* **119**, January, pp. 161–167.

[12] Castanier, M., Ottarson, G., and Pierre, C., 1997. "A reduced order modeling technique for mistuned bladed-disks". *Journal of Vibration Acoustics,* **119**(3), pp. 439–447.

[13] Yang, M., and Griffin, J., 1999. "A reduced order model of mistuning using a subset of nominal modes". *presented at the International Gas Turbine Institute Turbo Expo, Indianapolis,IN, ASME Paper 99-GT-288,* **39**.

[14] Feiner, D., and Griffin, J., 2002. "A fundamental model of mistuning for a single family of modes". *Journal of Turbomachinery,* **124**, October, pp. 507–605.

[15] Corral, R., Gallardo, J., and Vasco, C., 2004. "Linear stability analysis of lpt rotor packets – part ii: Tree-dimensional results and mistuning effects". *ASME Paper 2004-GT-54120.*

[16] Kielb, J., and Abhari, R., 2003. "Experimental study of aerodynamic and structural damping in a full-scale rotating turbine". *Journal of Engineering for Gas Turbines and Power,* **125**, January, pp. 102–112.

[17] Corral, R., López, C., and Vasco, C., 2004. "Linear stability analysis of lpt rotor packets – part i: Methodology and two-dimensional results". *ASME Paper 2004-GT-54119*.

[18] Wilkinson, J., 1988. *The Algebraic Eigenvalue Problem*. Oxford Science Publications.